Photonic Bloch oscillations in laterally confined Bragg mirrors

Alexey Kavokin and Guillaume Malpuech
LASMEA, Université Blaise Pascal Clermont-Ferrand II, 63177 Aubiere, France

Aldo Di Carlo and Paolo Lugli
Istituto Nazionale per la Fisica della Materia and Dipartimento di Ingegneria Elettronica, Università di Roma ''Tor Vergata,'' Via Tor Vergata, 110, I-00133 Roma, Italy

Fausto Rossi
INFM and Dipartimento di Fisica, Politecnico di Torino Corso Duca degli Abruzzi 24, 10129 Torino, Italy
(Received 20 September 1999)

We show that the photons in laterally confined Bragg mirrors may experience Bloch oscillations similar to those of electrons in semiconductor superlattices subjected to electric fields. An effective electric field is produced in the photonic case by variation of the lateral size of the structure as one moves along the structure axis. The temporal behavior of a short pulse of light oscillating within a miniband of such an optical superlattice made from the porous silicon has been modeled by a proper scattering-state simulation scheme.

Very recently the phenomenon of electron Bloch oscillations has been experimentally demonstrated in semiconductor superlattices.[1] The problem of the existence of such oscillations generated long and controversial debates since the 1950s when Wannier formulated the theory of electronic states within a crystal in the presence of a uniform electric field.[2–5] The theory has met much difficulties because of the problem of the unboundedness of the potential operator eFx (where e is an electron charge, F is an electric field, and x is a real space coordinate) and only recently a rigorous formalism has been developed.[6]

An electron in a crystal experiences Bloch oscillations if the dephasing time is longer than the oscillation time h/eFd, where d is the lattice period. Two main mechanisms responsible for the damping of Bloch oscillations are electron-phonon scattering and Zener tunneling.[5,7–10] For observation of Bloch oscillations a large supercell in real space, i.e., a large period d, is needed, which corresponds to a small Bloch-oscillation time. Moreover, there exists a limitation on the strength of the applied electric fields, since they induce Zener tunneling between adjacent crystal bands (or superlattice minibands). In fact, up to now Bloch oscillations have only been observed in semiconductor superlattices.

The analogy between an electron in a real crystal and a photon in a dielectric medium[11,12] allows us to speculate about a possibility of photonic Bloch oscillations in specially designed photonic crystals. Since photons have a much greater coherence length than electrons, they might appear to be better candidates for observation of the Bloch oscillations. In the recent studies[13,14] the photonic Stark ladder has been addressed. This report is aimed to demonstrate the existence of such oscillations in photonic crystals, namely in laterally confined Bragg mirrors.

The inset in Fig. 1 shows schematically the design of a model structure which we have chosen for studies of photonic Bloch oscillations. It is an optical superlattice (Bragg mirror) made from porous silicon with two different degrees of porosity. An effective electric field acting on photons is provided by a varying lateral confinement of the structure (unlike in Refs. 13 and 14 where the effective field was created by a variation of the refractive index). Porous silicon seems to be a very convenient material for our purposes because it allows altering of the refractive index in a wide range. The technology of growth of the Bragg mirrors from porous silicon is quite well developed,[15] and its chemical etching and metallization have become quite ordinary operations, at present. We have chosen the same refractive indices of two sorts of porous silicon as in Ref. 15 ($n_a = 1.27$ and $n_b = 2.25$). The corresponding layer thicknesses are $L_a = 380$ nm and $L_b = 300$ nm, respectively. The structure con-

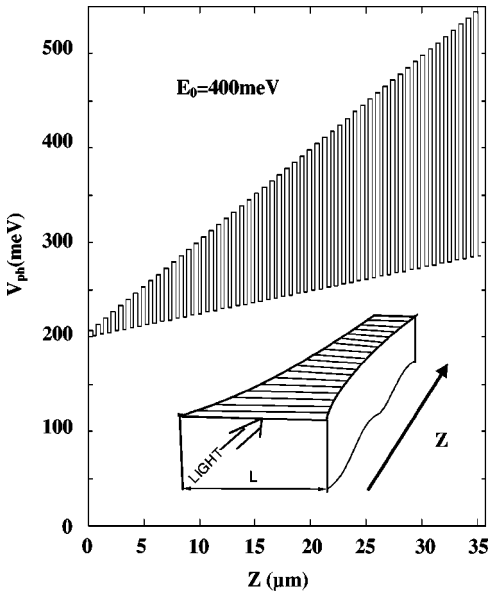

FIG. 1. The potential profile of the confined optical superlattice in its growth direction for a photon having an energy $E_0 = 400$ meV. The inset shows the scheme of the structure considered. The structure is periodical along the growth direction and confined in plane. The light is incident along the growth direction.

 ©2000 The American Physical Society

tained 46 periods. The variation of lateral dimension of the structure can be achieved by chemical etching. Then the etched surfaces should be metallized in order to achieve a required degree of the in-plane optical confinement. Further, we will suppose the electric field in the structure to have zeros at the metallized surfaces.

In this case, the photonic wave vector in the direction of light propagation can be defined as

$$k_{ph}=\sqrt{\left(\frac{nE}{\hbar c}\right)^2-\left(\frac{j\pi}{L}\right)^2}, \tag{1}$$

where E is the energy, n is the refractive index, L is the width of the waveguide, and j is the number of the confined photonic modes. Here, we suppose that the photon electric field in the structure can be factorized as a product of the plane wave propagating along the axis and the cosinelike envelope function in the direction of the lateral confinement (the adiabatic approximation). In the following we shall suppose $j=1$, for simplicity. If a pulse of light whose spectral width Δ is much less than $\hbar\pi nc/L$ is incident on the structure, one can write k_{ph} in the form

$$k_{ph}=\sqrt{\frac{2m_{ph}(E-V_{ph})}{\hbar^2}}, \tag{2}$$

where

$$V_{ph}=\frac{E_0}{2}+\frac{\hbar^2c^2}{2n^2E_0}\left(\frac{\pi}{L}\right)^2, \tag{3}$$

$$m_{ph}=\frac{n^2}{c^2}E_0, \tag{4}$$

and E_0 is the energy of the center of the pulse ($E_0\gg\Delta$).

For the sake of making the optical system analogous to the electronic superlattice subjected to the external electric field it is convenient to choose L in the form

$$L=\frac{\theta}{\sqrt{Q+z}}, \tag{5}$$

where θ and Q are constants, and $z=0$ corresponds to the beginning of the structure. In the model structure considered here $Q=680$ nm and $\theta=1.98\times10^5$ nm$^{3/2}$. For this particular geometry, we can rewrite

$$V_{ph}=\frac{E_0}{2}+\frac{\hbar^2c^2}{2n_j^2E_0}\left(\frac{\pi}{\theta}\right)^2Q+eF_{eff}z, \tag{6}$$

where

$$eF_{eff}=\frac{\hbar^2c^2}{2n_j^2E_0}\left(\frac{\pi}{\theta}\right)^2. \tag{7}$$

Here F_{eff} is an effective electric field acting on photons, and $j=a,b$ for two sorts of layers within the structure. The potential (6) is plotted in Fig. 1 for $E_0=400$ meV. In each type (a or b) of materials, the potential is a linear function of the coordinate near $E=E_0$ as it is in case of a conventional superlattice subject to an electric field. Note, however, that the value of the effective electric field is not the same in two sorts of layers we used. In material (a) we have $F=8.3\times10^3$ V/m, while in the material (b) $F=2.3\times10^3$ V/m. Also, the values of the potential and electric field seen by an incident photon depend on the energy of the photon, which is a peculiarity of our optical systems. The effect of the lateral confinement on the propagation of photons is strongly different in the high-index and low-index materials. Another difference from a conventional superlattice case is that the optical superlattice potential does not exceed the photon energy E_0 in most parts of the structure. This is less pronounced for low values of E_0, whereas the approximation $E_0\gg\Delta$ is better adapted for the large values of E_0. This specific complicates direct application of the existing theory of Bloch oscillations in a Stark superlattice to our system but does not affect the existence of the effect as we will see below.

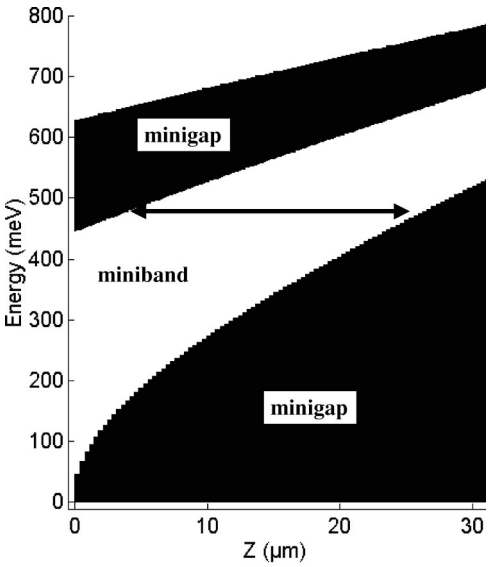

FIG. 2. Photonic band diagram of the confined optical superlattice in its growth direction. White regions represent the minibands; dark regions represent the minigaps.

The variation of n can also be used to model the electric field for photons.[13,14] However, one should take into account a strong effect of n on the photonic mass and on the slope of the potential curve.

The real miniband structure of our model sample along the direction of light propagation (z direction) is shown in Fig. 2. The allowed miniband energies have been found from the condition

$$-1\leqslant(t_{11}+t_{22})/2\leqslant1, \tag{8}$$

where t_{11} and t_{22} are the diagonal elements of the transfer matrix across the period of the structure

$$T_d=T_aT_b. \tag{9}$$

Here the matrix across a layer of width L_j with refractive index n_j has the form

$$T_j=\begin{bmatrix}\cos(k_jL_j) & \frac{i}{n_j}\sin(k_jL_j)\\ in_j\sin(k_jL_j) & \cos(k_jL_j)\end{bmatrix}, \tag{10}$$

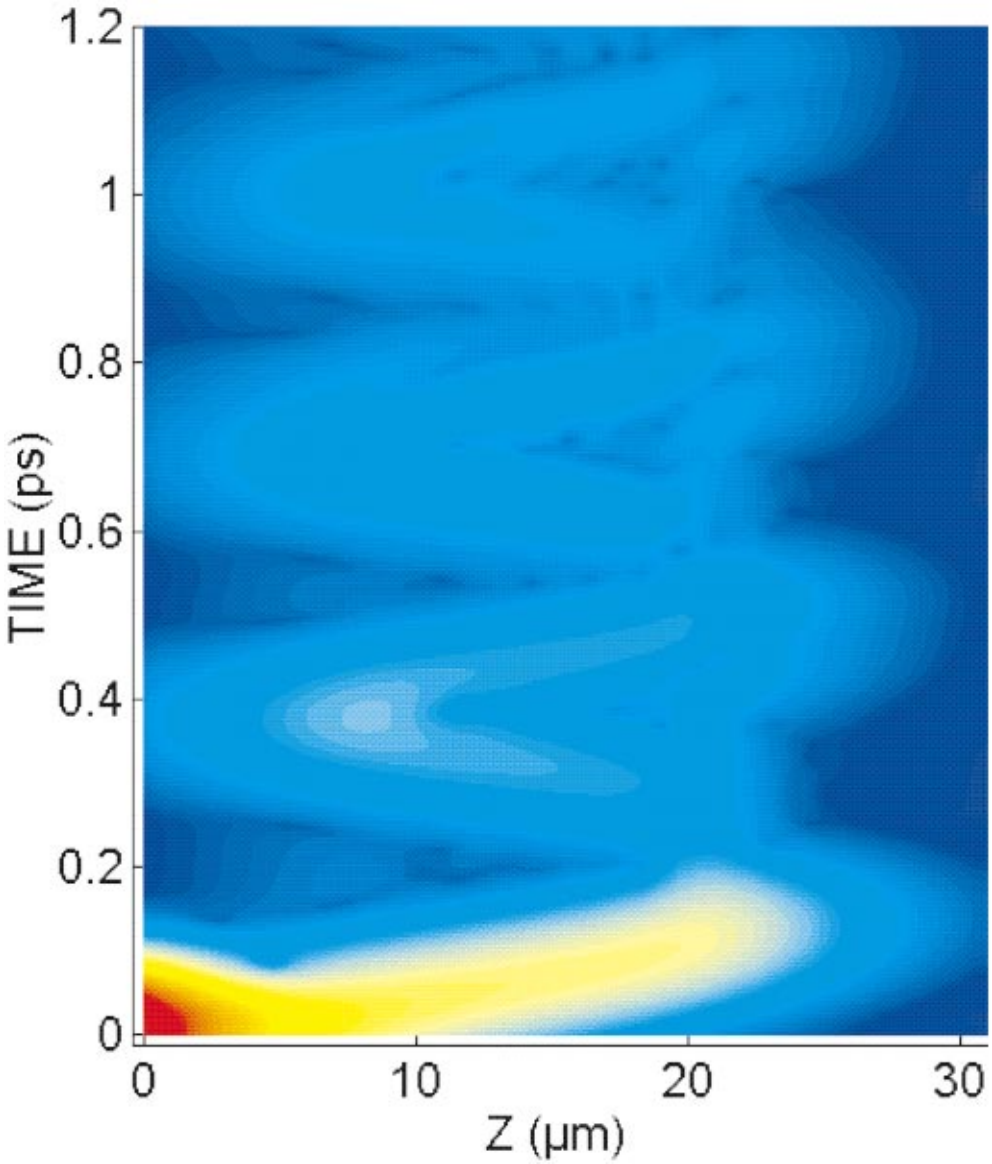

FIG. 3. (Color) Propagation of a Gaussian pulse of light in the confined optical superlattice. The color changes from blue to red proportionally with respect to the intensity of the electric field.

with k_j given by formula (1) where one must substitute the refractive index and the lateral confinement dimension which correspond to the given layer. Condition (8) follows from the Bloch theorem.

One can see inclined minibands and minigaps. Note that the energies of the band edges of photonic gaps change almost linearly with the coordinate which confirms the analogy with a conventional superlattice subject to an electric field applied along the growth direction. On the other hand, the inclination angle of minibands exceeds the effective electric field value given by Eq. (10). For the bottom of the first allowed miniband it yields $F=1.6\times10^4$ V/m. The difference between the slope of the bands and the effective field is not surprising since we are very far from the limit of a homogeneous superlattice with wide minibands assumed by a classical theory of Bloch oscillations.[2]

In order to study the temporary dynamics of a short light pulse confined within the miniband of our optical superlattice we have used a *scattering-state* technique.[16] The procedure requires a calculation of the scattering states $E_\omega(z,\omega)$ in the system in the case of incidence of a plane wave with a frequency ω and an amplitude equal to 1 at $z=0$. This field can be readily found by a transfer matrix method.[17] Within this method, each layer of the structure is characterized by a 2×2 matrix Eq. (10) connecting the in-plane components of electric and magnetic fields at the beginning and at the end of the layer. The transfer matrix T across entire the structure is a product of the transfer matrices across all the layers.

The amplitude reflection coefficient of the structure has a form

$$r(\omega)=\frac{n_i(T_{11}+T_{12}n_f)-(T_{21}+T_{22}n_f)}{n_i(T_{11}+T_{12}n_f)+(T_{21}+T_{22}n_f)}, \qquad (11)$$

where n_f is the refraction index in the last (semi-infinite) layer of the structure and T_{mn} denotes the elements of the matrix T. Now we can find the frequency-dependent electric field as

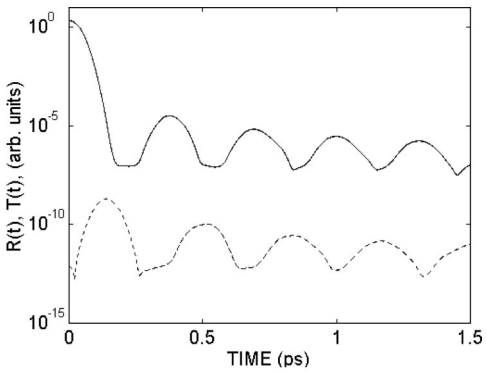

FIG. 4. Calculated time-resolved reflection (solid) and transmission (dashed) spectra of the confined Bragg mirror under study.

$$E_\omega(z,\omega)=T^z_{11}[1+r(\omega)]+T^z_{12}[1-n_i r(\omega)], \qquad (12)$$

where T^z is the transfer matrix from 0 to z. Finally, the time-dependent electric field can be found as

$$E(z,t)=\frac{1}{2\pi}\int d\omega e^{-i\omega t}E_\omega(z,\omega)f_\omega(\omega), \qquad (13)$$

where $f_\omega(\omega)$ is the spectral function of the incident pulse. We have chosen it in the form

$$f_\omega(\omega)=\frac{\hbar}{\sqrt{\pi}\Delta}\exp\left[-\left(\frac{\hbar\omega-E_0}{\Delta}\right)^2\right]. \qquad (14)$$

To summarize, we have represented the incident pulse as a linear combination of plane waves, have solved the wave equation for these plane waves by a transfer matrix technique, and have derived the time-dependent field in the system as a linear combination of solutions for individual plane waves.

Our pulse parameters are $E_0=530$ meV and $\Delta=45$ meV. Figure 3 shows the calculated electric field induced by the incident pulse in the structure as function of time and of the coordinate in the growth direction. The darkness of color on the figure is proportional to the electric field intensity. One can see an initial decrease of the intensity of the pulse when it tunnels through the minigap region ($0<z<3$ μm), and then the oscillations start between approximately $z=2$ μm and $z=25$ μm. Indeed, these are the Bloch oscillations of light within the inclined miniband. Note that the inclined minigap in the beginning of the structure filters the low-frequency wing of the pulse which mostly participates in oscillations.

As follows from Fig. 3 the period of observed Bloch oscillations of light is about $T=0.35$ ps. The classical formula

$$T=h/eFd, \qquad (15)$$

with an electric field $F=1.6\times10^4$ V/m obtained from the band diagram in Fig. 3, yields $T=0.38$ ps, which is in agreement with numerical symulations.

Experimentally, the photonic Bloch oscillations can be observed in time-resolved reflection and transmission spectra, as one can see from Fig. 4. The calculation has been performed according Eq. (13) with $z=0$ and $z=31.28$ μm for reflection and transmission spectra, respectively. Quite clear and pronounced oscillations are seen both in time-resolved reflection (solid) and transmission (dashed).

In conclusion, the formalisms describing electronic and optical Bloch oscillations are rather different, while indeed the photonic Bloch oscillations have the same physical nature as electronic ones and they can be observed in laterally confined periodical structures. Alternative structures suitable for observation of photonic Bloch ocsillations could be photonic wires with a cross section varying along the wire axis.

A.K. gratefully acknowledges the Instituto Nazionale della Fisica della Materia and the University of Rome II ''Tor Vergata'' for support during his stay in Rome.

[1] C. Waschke *et al.*, Phys. Rev. Lett. **70**, 3319 (1993); T. Dekorsky *et al.*, Phys. Rev. B **51**, R17 275 (1995).
[2] G. H. Wannier, Phys. Rev. **100**, 1227 (1955); **101**, 1835 (1956); **117**, 432 (1960); Rev. Mod. Phys. **34**, 645 (1962).
[3] J. Zak, Phys. Rev. Lett. **20**, 1477 (1968); Phys. Rev. **181**, 1366 (1969).
[4] D. Emin and C. F. Hart, Phys. Rev. B **36**, 7353 (1987); **41**, 3859 (1990); **43**, 2426 (1991); **43**, 4521 (1991).
[5] A. Di Carlo, P. Vogl, and W. Pötz, Phys. Rev. B **50**, 8358 (1994).
[6] G. Nenciu, Rev. Mod. Phys. **63**, 91 (1991).
[7] A. Sibille, J. F. Palmier, and F. Laruelle, Phys. Rev. Lett. **80**, 4506 (1998).
[8] G. von Plessen *et al.*, Phys. Rev. B **49**, R14 058 (1994).
[9] F. Rossi *et al.*, Phys. Rev. B **51**, 16 943 (1995).
[10] F. Rossi, A. Di Carlo, and P. Lugli, Phys. Rev. Lett. **80**, 3348 (1998).
[11] J. D. Joannopoulos, R. D. Meade, and J. N. Winn, *Photonic Crystals* (Princeton University Press, Princeton, NJ, 1995).
[12] J. N. Winn *et al.*, Phys. Rev. B **59**, 1551 (1999).
[13] G. Monsivais, M. del Castillo-Mussot, and F. Claro, Phys. Rev. Lett. **64**, 1433 (1990).
[14] C. Martijn de Sterke *et al.*, Phys. Rev. E **57**, 2365 (1998).
[15] L. Pavesi, G. Panzarini, and L. C. Andreani, Phys. Rev. B **58**, 15 794 (1998).
[16] J. E. G. Farina, in *International Encyclopedia of Physical Chemistry and Chemical Physics*, edited by R. McWeeny (Pergamon, Oxford, 1975), Topic 2, Vol. 1.
[17] M. Born and E. Wolf, *Principles of Optics* (Pergamon, Oxford, 1980).